WEES-2020 Special Issue

J. Indian Chem. Soc.,
Vol. 97, No. 10b, October 2020, pp. 1973-1982

Modeling and analysis of multiphase induction generator used in AC and DC hybrid micro-grid generating system

Saikat Ghosh* and S. N. Mahato

Department of Electrical Engineering, National Institute of Technology Durgapur, Durgapur-713 209, West Bengal, India

E-mail: saikatghosh1407@gmail.com

Manuscript received online 31 May 2020, revised and accepted 06 August 2020

This paper presents the dynamic modeling and control strategy of a multi-phase (six-phase) induction generator to utilize it as a stand-alone electrical power sources in collaboration with a hydro energy source. This proposed system can supply AC and DC power simultaneously with the help of two different three-phase windings. The first three-phase winding is known as power winding which supplies power to AC load through a controlled cyclo-converter as a constant frequency AC output and second three-phase winding, known as control winding, supplies power to DC load through a static excitation regulator. An energy storing device is installed in DC side winding for increasing the reliability of this micro-grid generating system. Simulated results contain transient and steady state analysis of multi-phase induction generator for voltage build up at no load and different types of load switching in both AC and DC sides. The provided MATLAB/Simulink based prototype model of this proposed generating system ensures that stand-alone multi-phase induction generator works satisfactorily for supplying both controlled AC and DC power to load simultaneously.

Keywords: Multi-phase induction generator, AC and DC hybrid micro-grid, hydro power, renewable energy source, control strategy.

1. Introduction

Presently the whole world is suffering from two major problems - one is energy crisis and another is pollution. For this problem, renewable energy, such as small hydro, solar, wind etc., is one of the finest and probably the only solution[1]. Till now, in India, more than 4 crore households are un-electrified, because they are situated in such a remote rural area where national grid is unavailable. But research finds out that 80% of that area has a high potential in renewable energy generation. For these areas, renewable energy based micro-grid is the best solution due to its several advantages like less maintenance, almost zero running cost etc.[2–5]. Here, a hybrid micro-grid has been proposed for supplying AC and DC load simultaneously.

Mainly induction generators are used for extracting power from different renewable energy sources like small hydro, wind etc. for several advantages like simple construction, low cost, ruggedness, high reliability and low maintenance. In the recent time, multiphase induction generators (more than 3 phases) gain a large interest for the application of variable speed drive electric system due to several advantages of it when compared with conventional three-phase system[6–7]. It is capable to increase the net amount of power while maintaining the per phase power rating same as previous with ease. However, till now, multi-phase induction motor based research works have been carried out more successfully as compared to multi-phase induction generator. This multi-phase induction generator is very much suitable for extracting power through small hydro or wind energy in remote area. Multi-phase induction generator consists of two different three-phase windings sets, which is under the same magnetic field. Modeling, steady state and transient analysis for different types of load, excitation control and performance analysis are discussed in detail[8–11]. By using indirect field oriented control a constant frequency AC voltage is generated in power winding for supplying power to the AC load and a controlled DC power is generated in controlled winding for supplying the power to DC load. By implementation of

J. Indian Chem. Soc., Vol. 97, No. 10b, October 2020

bidirectional energy flow, the number of converter is reduced and system complexity is also reduced to a great extent[12–14].

This paper presents the modeling, analysis and control strategy of a multi-phase induction generator used in AC and DC hybrid micro-grid generating system. This entire paper is sub-divided in the following sections: A brief discussion about the proposed system topology is done in Section 2. Section 3 contains detail mathematical modeling of proposed multi-phase induction generator. The control strategy for the both AC and DC side power windings are discussed in Section 4 and Section 5 presents the simulation model and results. Conclusion is given in Section 6.

2. System topology

Fig.1 represents the entire structure of proposed standalone AC and DC hybrid micro-grid generating system consisting of a multi-phase induction generator. A cross flow turbine extracts power from the hydro energy and the power is fed to multi-phase induction generator as an energy input. Two three-phase sets of winding are placed inside of the rotor. One of these three-phase winding is known as power winding that delivers constant frequency AC power to the AC side load via a control unit which contains a cyclo-converter[15]. Second three-phase windings is known as control winding that delivers DC power to DC side load via a static excitation regulator (Bidirectional converter). As per the DC side reference value, a pulse is generated by control unit of DC side and fed to static excitation regulator. DC side also contains an energy storage element i.e. battery for storing energy when there is excess power generation by surplus amount of water. However, when there is not sufficient amount of water, then the energy is supplied from battery towards AC load through bidirectional converter and bypass switch. The number of poles of these two sets of three-phase windings is same and they are electrically isolated from each other but they work under same magnetic field[16–17]. That's why this system has higher electromagnetic compatibility, great performance and high standard power output among one another and are short circuited by end ring[18–21].

3. Mathematical modeling

The schematic outline of two different three-phase stator winding sets and one rotor winding for a multi-phase induction generator are given in the Fig. 2. These star-connected both sets of three-phase stator windings are named as XYZ and ABC, and they are displaced by an arbitrary angle α. Each phase of XYZ and ABC windings are displaced by an angle of 120°. The rotor windings are also displaced by 120°,

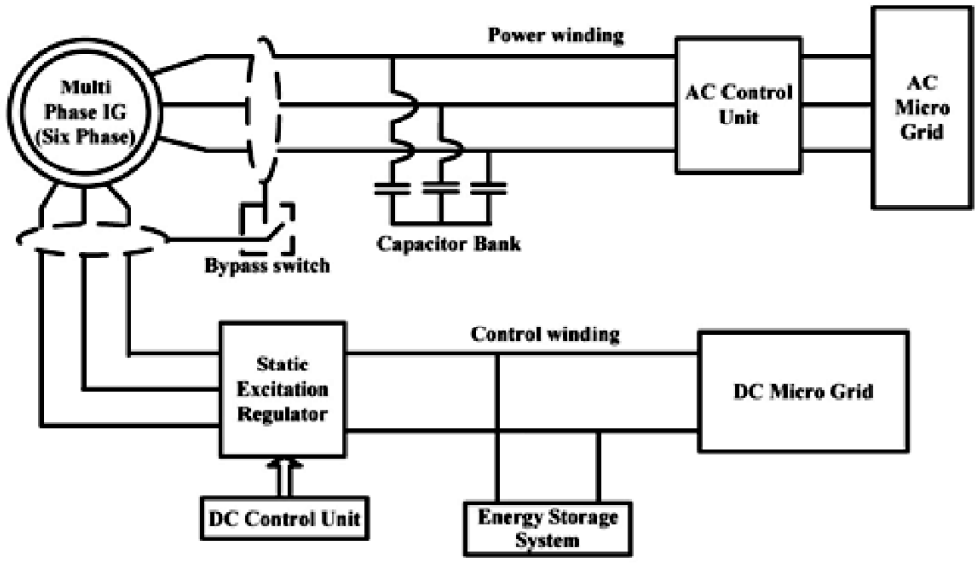

Fig. 1. Structure of proposed stand-alone AC and DC hybrid micro-grid generating system based on multi-phase induction generator.

which are denoted by ar, br, cr.

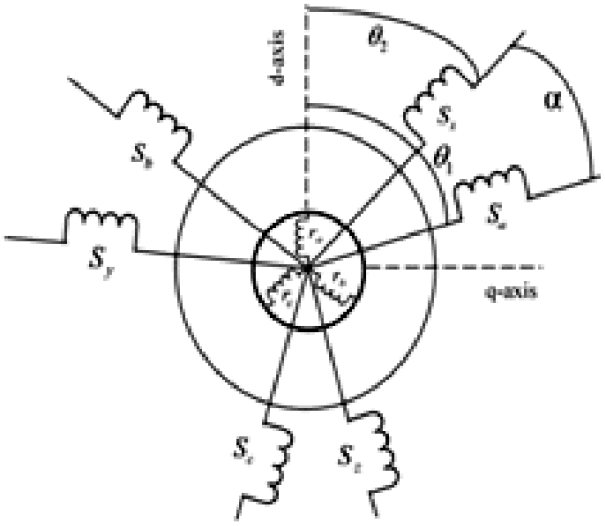

Fig. 2. Schematic diagram of winding distribution of multi-phase induction generator.

An arbitrary reference frame is taken for modeling the multi-phase induction generator. Depending on this arbitrary reference frame, the voltage equations express as

$$V_{d1} = -R_1 I_{d1} + P\lambda_{d1} - \omega_k \lambda_{q1} \quad (1)$$

$$V_{q1} = -R_1 I_{q1} + P\lambda_{q1} - \omega_k \lambda_{d1} \quad (2)$$

$$V_{d2} = -R_2 I_{d2} + P\lambda_{d2} - \omega_k \lambda_{q2} \quad (3)$$

$$V_{q2} = -R_2 I_{q2} + P\lambda_{q2} - \omega_k \lambda_{d2} \quad (4)$$

$$V_{dr} = 0 = R_r I_{dr} + P\lambda_{dr} - (\omega_k - \omega_r)\lambda_{qr} \quad (5)$$

$$V_{qr} = 0 = R_r I_{qr} + P\lambda_{qr} + (\omega_k - \omega_r)\lambda_{dr} \quad (6)$$

In this above equation, ω_k and ω_r represent the speeds of the arbitrary reference frame and rotor respectively. P denotes derivative with respective of time and the all other symbols represent their as usual meanings. The flux linkage equations can be written as:

$$\lambda_{d1} = -L_1 I_{d1} - L_{lm}(I_{d1} + I_{d2}) + L_{dq} I_{q2} + L_m(-I_{d1} - I_{d2} + I_{dr}) \quad (7)$$

$$\lambda_{q1} = -L_1 I_{q1} - L_{lm}(I_{q1} + I_{q2}) + L_{dq} I_{d2} + L_m(-I_{q1} - I_{q2} + I_{qr}) \quad (8)$$

$$\lambda_{d2} = -L_2 I_{d2} - L_{lm}(I_{d1} + I_{d2}) - L_{dq} I_{q1} + L_m(-I_{d1} - I_{d2} + I_{dr}) \quad (9)$$

$$\lambda_{q2} = -L_2 I_{q2} - L_{lm}(I_{q1} + I_{q2}) + L_{dq} I_{d1} + L_m(-I_{q1} - I_{q2} + I_{qr}) \quad (10)$$

$$\lambda_{dr} = L_r I_{dr} + L_m(-I_{d1} - I_{d2} + I_{dr}) \quad (11)$$

$$\lambda_{qr} = L_r I_{qr} + L_m(-I_{q1} - I_{q2} + I_{qr}) \quad (12)$$

There is common mutual inductance (L_{lm}) between two sets of stator windings because they are sharing same stator slots. L_{dq} represents cross saturation coupling between d-q axis of the stator. L_m represents the mutual inductance between stator and rotor. Based on the above equation, an equivalent circuit is developed in Fig. 3.

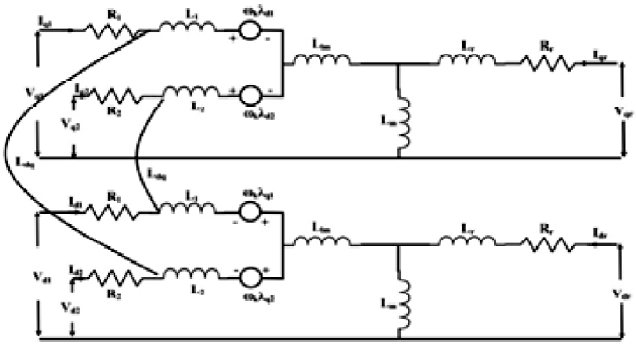

Fig. 3. Equivalent circuit diagram of multi-phase induction generator.

The current expressions can be develop from the above equation of flux linkage.

$$I_{q1} = (1/L)\begin{bmatrix}\lambda_{q1}(L_2 + L_{lm}) - \lambda_{mq} L_2 - L_{lm}\lambda_{q2} \\ + L_{dq}(\lambda_{d2} - \lambda_{md})\end{bmatrix} \quad (13)$$

$$I_{q2} = (1/L)\begin{bmatrix}\lambda_{q2}(L_1 + L_{lm}) - \lambda_{mq} L_1 - L_{lm}\lambda_{q1} \\ - L_{dq}(\lambda_{d1} - \lambda_{md})\end{bmatrix} \quad (14)$$

$$I_{d1} = (1/L)\begin{bmatrix}\lambda_{d1}(L_2 + L_{lm}) - \lambda_{md} L_2 - L_{lm}\lambda_{d2} \\ - L_{dq}(\lambda_{q2} - \lambda_{mq})\end{bmatrix} \quad (15)$$

$$I_{d2} = (1/L)\begin{bmatrix}\lambda_{d2}(L_1 + L_{lm}) - \lambda_{md} L_1 - L_{lm}\lambda_{d1} \\ + L_{dq}(\lambda_{q1} - \lambda_{mq})\end{bmatrix} \quad (16)$$

$$I_{qr} = (\lambda_{qr} - \lambda_{mq})/L_r \quad (17)$$

$$I_{dr} = (\lambda_{dr} - \lambda_{md})/L_r \quad (18)$$

Now these values of currents are substituted in voltage eqs. (1) to (6) and the equations are modified as given in eqs. (19) to (24).

$$P\lambda_{q1} = V_{q1} - \omega_k\lambda_{d1} - (R_1/L)$$
$$\left[\lambda_{q1}(L_2 + L_{lm}) - \lambda_{mq}L_2 - L_{lm}\lambda_{q2} - L_{dq}(\lambda_{d2} - \lambda_{md})\right] \quad (19)$$

$$P\lambda_{d1} = V_{d1} + \omega_k\lambda_{q1} - (R_1/L)$$
$$\left[\lambda_{d1}(L_2 + L_{lm}) - \lambda_{md}L_2 - L_{lm}\lambda_{d2} - L_{dq}(\lambda_{q2} - \lambda_{mq})\right] \quad (20)$$

$$P\lambda_{q2} = V_{q2} - \omega_k\lambda_{d2} - (R_2/L)$$
$$\left[\lambda_{q2}(L_1 + L_{lm}) - \lambda_{mq}L_1 - L_{lm}\lambda_{q1} - L_{dq}(\lambda_{d1} - \lambda_{md})\right] \quad (21)$$

$$P\lambda_{d2} = V_{d2} + \omega_k\lambda_{q2} - (R_2/L)$$
$$\left[\lambda_{d2}(L_1 + L_{lm}) - \lambda_{md}L_1 - L_{lm}\lambda_{d1} - L_{dq}(\lambda_{q1} - \lambda_{mq})\right] \quad (22)$$

$$P\lambda_{qr} = -(\omega_k - \omega_r)\lambda_{dr} - (R_r/L_r)(\lambda_{qr} - \lambda_{mq}) \quad (23)$$

$$P\lambda_{dr} = (\omega_k - \omega_r)\lambda_{qr} - (R_r/L_r)(\lambda_{dr} - \lambda_{md}) \quad (24)$$

where,

$$\lambda_{mq} = A\left[(1/L)\left\{\begin{matrix}(\lambda_{q1}L_2 + \lambda_{q2}L_1)\\ + L_{dq}(\lambda_{d2} - \lambda_{d1})\end{matrix}\right\} + (\lambda_{qr}/L_r)\right] \quad (25)$$

$$\lambda_{md} = A\left[(1/L)\left\{\begin{matrix}(\lambda_{d1}L_2 + \lambda_{d2}L_1)\\ + L_{dq}(\lambda_{q2} - \lambda_{q1})\end{matrix}\right\} + (\lambda_{dr}/L_r)\right] \quad (26)$$

$$A = \left[1/\{(1/L_m) + (L_1 + L_2)/L + (1/L_r)\}\right] \quad (27)$$

$$L = L_1L_2 + L_1L_{lm} - L_2L_{lm} \quad (28)$$

The electromagnetic torque and rotor dynamic equations can be expressed in d-q axes as:

$$T_{cm} = (3/2)(p/2)(L_m/L_r)$$
$$[(I_{q1} + I_{q2})\lambda_{dr} - (I_{d1} + I_{d2})\lambda_{qr}] \quad (29)$$

$$\omega_r/\omega_b = (1/P)(1/\omega_b)(p/2)(1/J)(T_{cm} - T_{sh}) \quad (30)$$

where T_{sh} is known as torque of the shaft, p denotes the pole number, moment of inertia express as J, ω_b denoted as base speed express in rad/sec.

The L_m is known as magnetizing inductance which based on the saturation degree and this is non-linear with magnetizing current I_m. That is why it can be expressed as:

$$I_m = \sqrt{\left\{(-I_{q1} - I_{q2} + I_{qr})^2 + (-I_{d1} - I_{d2} + I_{dr})^2\right\}} \quad (31)$$

$$L_m = A_1 + A_2I_m + A_3I_m^2 + A_4I_m^3 \quad (32)$$

Appendix contains the value of A_1, A_2, A_3, and A_4.

3.1. Modeling of shunt excitation capacitor:

Two different capacitors C_{sh1} and C_{sh2} are attached in both sets of stator windings. The three-phase voltage and current equations of shunt excitation capacitor are converted in d-q axes with the help of Krause Transformation as given below:

$$PV_{q1} = (I_{q1c}/C_{sh1}) - (\omega_bV_{d1}) \quad (33)$$
$$PV_{d1} = (I_{d1c}/C_{sh1}) + (\omega_bV_{q1}) \quad (34)$$
$$PV_{q2} = (I_{q2c}/C_{sh2}) - (\omega_bV_{d2}) \quad (35)$$
$$PV_{d2} = (I_{d2c}/C_{sh2}) - (\omega_bV_{q2}) \quad (36)$$

In this above equation I_{q1c}, I_{d1c} and I_{q2c}, I_{d2c} are the current components of q-d axes excitation capacitor for the stator winding set I and set II respectively. At the time of switching the load, the voltage regulation is not up to the mark only with shunt excitation capacitor. That is why series excitation capacitor is also inserted in the load terminal of multi-phase induction generator.

3.2. Modeling of series excitation capacitor:

There are two capacitors C_{se1} and C_{se2}which are connected in series with load. As a result, the current flow through capacitor is same as the load current. The voltages across the series capacitors in d-q axes are determined by load current and expressed as given below:

$$PV_{q1se} = I_{q1L}/C_{se1} \quad (37)$$
$$PV_{d1se} = I_{d1L}/C_{se1} \quad (38)$$
$$PV_{q2se} = I_{q2L}/C_{se2} \quad (39)$$
$$PV_{d2se} = I_{d2L}/C_{se2} \quad (40)$$

The load voltage can now be written as:

$$V_{q1L} = V_{q1} - V_{q1se} \quad (41)$$
$$V_{d1L} = V_{d1} - V_{d1se} \quad (42)$$
$$V_{q2L} = V_{q2} - V_{q2se} \quad (43)$$
$$V_{d2L} = V_{d2} - V_{d2se} \quad (44)$$

3.3. Modeling of static load:

Let resistive loads of R_1 and R_2 connected across the load terminals of two sets of stator windings - Set I and Set II respectively. So load current can be written as:

$$I_{d1L} = V_{d1L}/R_1 \quad (45)$$

$$I_{q1L} = V_{q1L}/R_1 \quad (46)$$

$$I_{d2L} = V_{d2L}/R_2 \quad (47)$$

$$I_{q2L} = V_{q2L}/R_2 \quad (48)$$

By applying KCL at the terminal of capacitor, the current passing across shunt capacitor can be expressed as given below:

$$I_{q1C} = I_{q1} - I_{q1L} \quad (49)$$

$$I_{d1C} = I_{d1} - I_{d1L} \quad (50)$$

$$I_{q2C} = I_{q2} - I_{q2L} \quad (51)$$

$$I_{d2C} = I_{d2} - I_{d2L} \quad (52)$$

$$PV_{q1} = (I_{q1}/C_{sh1}) - \{V_{q1}/(R_1C_{sh1})\} - \omega_b V_{d1} \quad (53)$$

$$PV_{d1} = (I_{d1}/C_{sh1}) - \{V_{d1}/(R_1C_{sh1})\} - \omega_b V_{q1} \quad (54)$$

$$PV_{q2} = (I_{q2}/C_{sh2}) - \{V_{q2}/(R_2C_{sh2})\} - \omega_b V_{d2} \quad (55)$$

$$PV_{d2} = (I_{d2}/C_{sh2}) - \{V_{d2}/(R_2C_{sh2})\} - \omega_b V_{q2} \quad (56)$$

4. Control strategy

For simultaneous generation and supply of AC and DC power from this proposed generating system, two different and independent control strategies are described here. One of them is known as AC side control unit which is used for getting constant frequency output towards AC side load and another one is known as DC side control unit which is used for getting constant DC output voltage towards DC side load[22,23].

4.1. AC side control:

Fig. 4 represents the schematic diagram of control strategy for the constant frequency AC power generation by multiphase induction generator through capacitor bank. Due to the change in load and the variation of turbine speed, the supply frequency is fluctuating in nature[24–26]. This problem can be overcome by using this proposed system. As a first step of control, actual frequency of generated AC power is detected by frequency analyzer circuit and that detected signal is fed to saw-tooth generator. A saw-tooth signal is generated and compared with the actual signal to generate 12 pulses, which are fed to cyclo-converter.

With the help of this pulse controlled cyclo-converter, the proposed system will produce a constant frequency AC supply.

4.2. DC side control:

Fig. 5 represents the schematic diagram for the generating and controlling topology of DC side power generation by multi-phase induction generator. An assumption is taken in the account that DC side three-phase winding terminal voltage vector direction is same as d-axis and is perpendicular to q-axis of d-q rotating reference frame[27,28]. At first, the terminal voltage and current of multi-phase induction generator are measured by measurement module. The value of ωt can be found out with the help of measured voltage through Phase lock loop (PLL). The three-phase measured current is con-

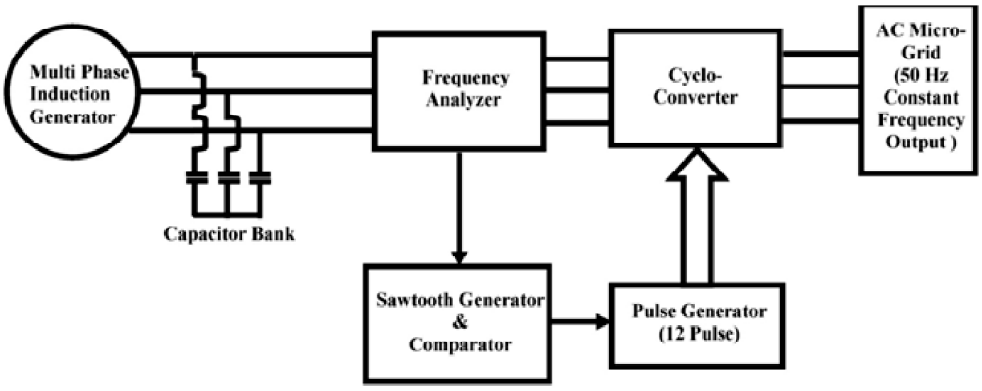

Fig. 4. Control topology for AC side power generation.

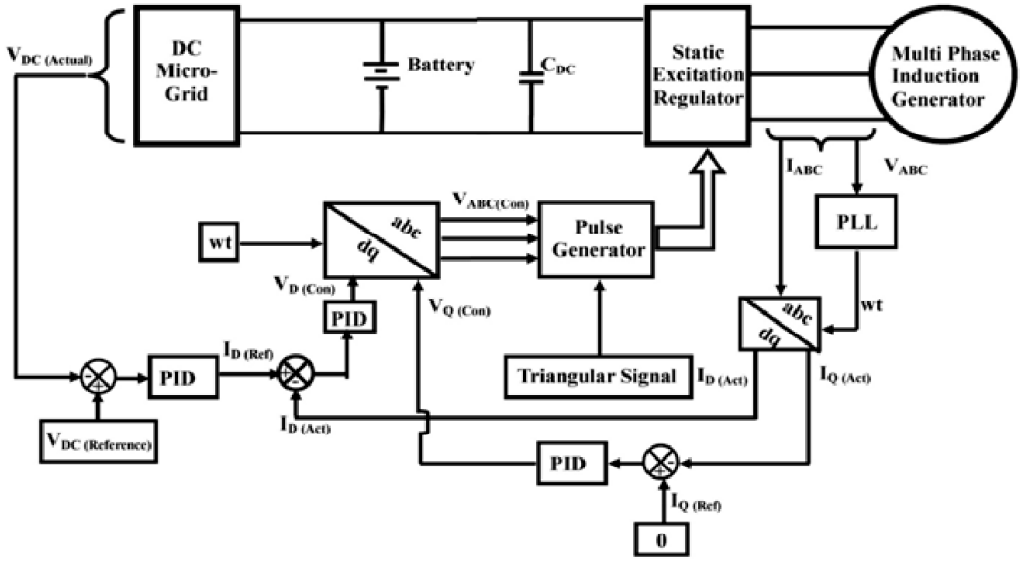

Fig. 5. Control topology for DC side power generation.

verted to d-q axes actual current through abc-dq transformation with the help of calculated ωt. The difference among the actual value and reference value of V_{DC} is converted to d-axis reference current (I_{DC}) through PID controller. The d-axis voltage $V_{D(con)}$ and q axis voltage $V_{Q(con)}$ are generated by the error signal in between d-q axes reference and actual current through PID controller. This controlled d-q axes voltage is converted to control three-phase voltage by dq-abc transformation with the help of calculated ωt. Nowa triangular signal is compared with this controlled three-phase voltages to generate pulses which are fed to static excitation controller for generating controlled DC power from AC power source. DC side capacitor and the energy storing elements like battery are used respectively for purifying the DC voltage and storing the DC power before feeding to DC side load.

5. Simulation results

A detailed theoretical modeling of AC and DC hybrid micro-grid system, which contains a multi-phase induction generator, static excitation regulator and controller for both sides are established in MATLAB/SIMULINK software. This type of induction generator has a unique construction and on the basis of its mathematical equations, a MATLAB model is developed. The static excitation regulator is connected to DC side winding for providing required reactive power for stable operation and better voltage regulation of the generating system while AC side winding generates AC power directly. The MATLAB model of both side controllers is designed as per proposed control methodology. AC side controller makes a constant frequency output from a variable frequency input with the help of a closed loop cyclo converter, while DC side controller tracks the reference value and feeds pulses to static excitation regulator for maintaining a stable operation of the proposed system.

This developed MATLAB simulation model is tested under various conditions like no load voltage build-up, switching of a sudden load with and without capacitor compensation in series, stable and constant frequency operation under variable speed drive, DC voltage conversion etc. This entire model is developed to generate 50 Hz, 340 V AC voltage in AC side winding and 480 V DC voltage in DC side winding of multi-phase induction generator. All the parameters are given in Appendix.

5.1. No-load voltage build-up:

Figs. 6, 7 and 8 show the no-load voltage waveforms of both sets of three-phase windings and DC voltage respectively. A delta connected per phase shunt excitation capacitor of 70 μF is used for this purpose of simulation. This proposed generating system generates a line to line voltage of 340 V at the rated speed of 1500 r.p.m. in both the set of

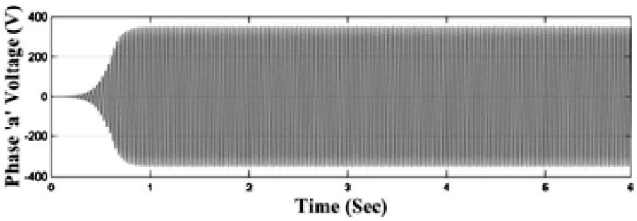

Fig. 6. No-load voltages build up in phase 'a'.

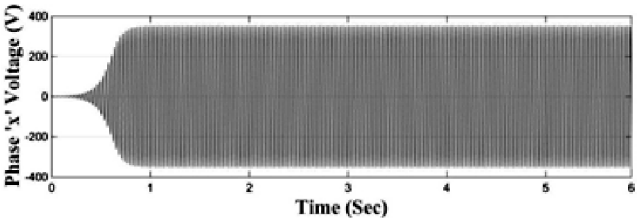

Fig. 7. No-load voltages build up in phase 'x'.

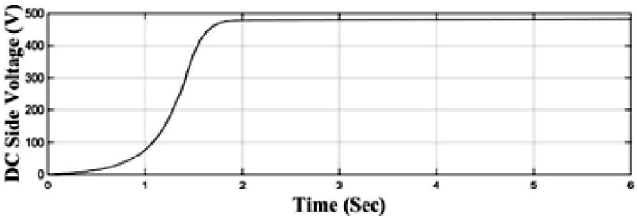

Fig. 8. No-load DC side generated voltage from SER.

three-phase winding. From the simulation results it is found that the voltages, at very initial stage, are very small before reaching their steady state values. From this simulation experiment it is noticed that the no-load voltage build up depends directly on the value of shunt excitation capacitor. The output from the static excitation regulator generates a 480 V DC from three-phase AC power at no load condition. By this entire analysis of no-load condition, it can be concluded that static performance of this proposed generating system is good.

5.2. Switching of load without series capacitor compensation:

Now transient analyses are carried out in this developed simulated model of proposed system by sudden switching of a load of 600 Ω at time t = 3 s in the AC side winding. From the simulation results, it can be observed that, the terminal voltages of AC side winding are reduced to 200 V at the time of switching of load as shown in Figs. 9 and 10. As a result, excitation currents of shunt capacitors are also reduced after switching of load as shown in Figs. 13 and 14. By the investigation of simulated results, it can be concluded that the voltage regulation of proposed system is poor when only shunt excitation capacitor is used. For the better voltage regulation of this system, series compensator is inserted in each line which will increases the reactive power supply with load and thus, improves the voltage profile.

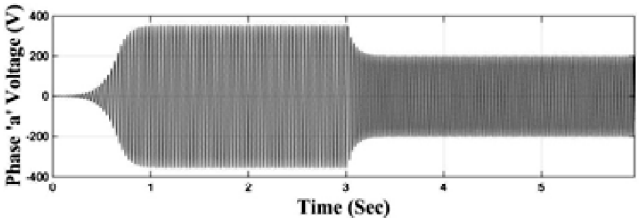

Fig. 9. Voltage of phase 'a' with a load switching time = 3 s.

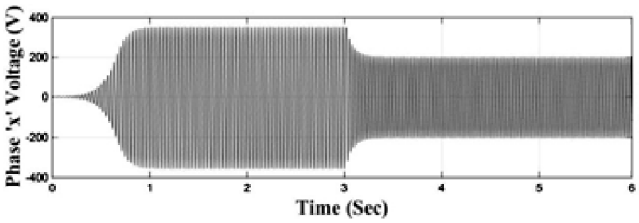

Fig. 10. Voltage of phase 'x' with a load switching time = 3 s.

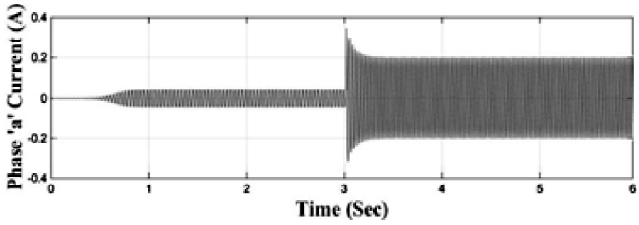

Fig. 11. Current of phase 'a' with a load switching time = 3 s.

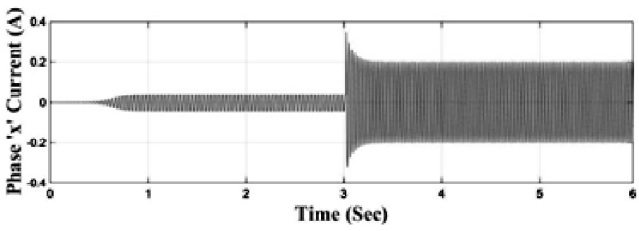

Fig. 12. Current of phase 'x' with a load switching time = 3 s.

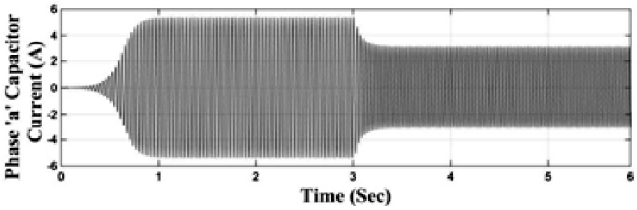

Fig. 13. Capacitor current of phase 'a' with a load switching time = 3 s.

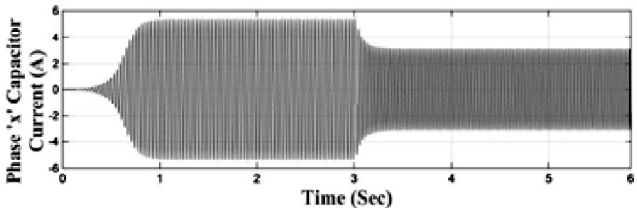

Fig. 14. Capacitor current of phase 'x' with a load switching time = 3 s.

5.3. Sudden switching of load with series compensation:

A 210 μF capacitor is connected in series with each terminal of the two sets of three phase winding for series compensation. In this series compensated condition, when the same amount of 600 Ω load is switched at time *t* = 3 s, then the voltage after switching the load remains almost same as no-load voltage build up because of reactive power compensation by series capacitor which are shown in Figs. 15 and 16. It is also find out that the magnitude of generated voltage before connecting the load is higher compared to no-load generated voltage without series compensation because of series capacitors which are already in the system before switching the load.

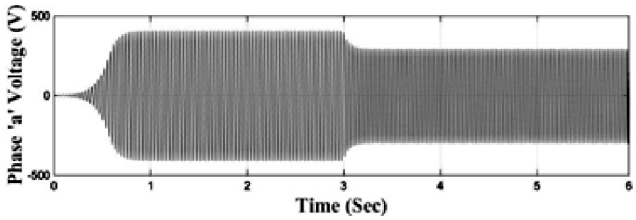

Fig. 15. Voltage of phase 'a' with a load switching time = 3 s.

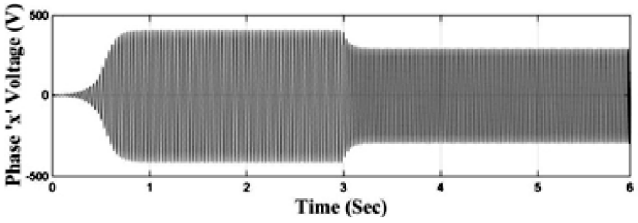

Fig. 16. Voltage of phase 'x' with a load switching time = 3 s.

5.4. AC side controlled output power with variable rotor speed:

The rotor speed may vary due to several reasons like turbine speed variation, sudden change of load, different kinds of faults etc. This speed change directly affects the frequency of generated power in AC side. For the variation of frequency of generated voltage with the variation of rotor speed is shown in Fig. 17. But the output voltage waveform with control circuit which contains a cyclo converter, gives a constant frequency voltage output as in shown Fig. 18. As a conclusion it can be says that the developed control circuit successfully converts variable frequency generated power to constant frequency power.

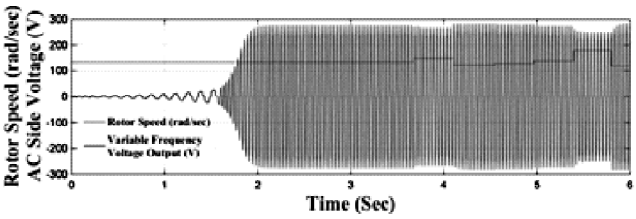

Fig. 17. Varying frequency voltage generation with the change of rotor speed.

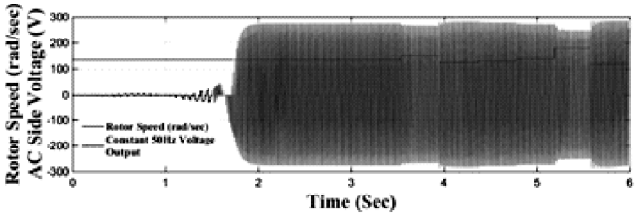

Fig. 18. Constant frequency voltage generation with the varying rotor speed.

5.5. DC side simulation:

A load of 200 Ω is suddenly switched at time *t* = 3 s across the DC side terminals, which is converted with the help of a static excitation regulator from the generated three-phase AC power. These simulated results are shown in Figs. 19 and 20. It is found that after switching the load, the terminal voltage is same as no-load generated voltage. An 1800 μF capacitor is used in DC side for purifying the generated DC before feeding it to load and energy storing elements.

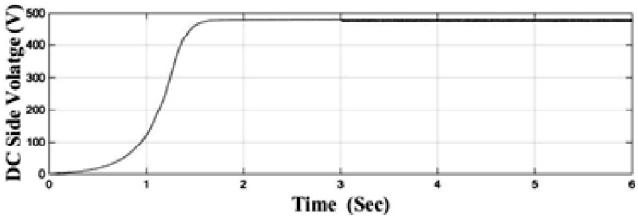

Fig. 19. Voltage of DC side with a load switching time = 3 s.

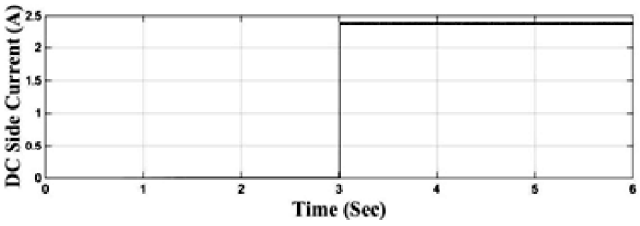

Fig. 20. Current of DC side with a load switching time = 3 s.

Conclusion

This paper represents the dynamic modeling, analysis and control strategy of a multi-phase (six-phase) induction generator to utilize it as an AC and DC hybrid electrical power source in collaboration with a hydro energy source. This proposed model can supply both AC and DC power simultaneously to different types of loads. This system is also very much reliable and highly efficient by enabling bi-directional energy flow and use of energy storing elements. For execution of proposed model, first multi-phase induction generator is modelled on the basis of its mathematical equations. For supplying AC and DC loads simultaneously, two different control strategies are proposed for both AC and DC sides. According to its mathematical equations and proposed control strategy, a MATLAB simulation model is developed. The steady-state and transient behavior of the generator have been studied. As a conclusion from the simulation results it can be says that generator has very good voltage regulation due to series compensation. The generating system can provide constant frequency output voltage. Moreover, in case of exigency, power from energy storing element can be diverted to AC side. Hence, the feasibility of this proposed hybrid AC and DC power generating system and the perfection of control strategies are proved. The hardware prototype of this proposed generating system will be implemented as a future course of action.

Appendix

Parameters		Values
Stator (ABC phase) resistance (R_1)		4.12 Ω
Stator (XYZ phase) resistance (R_2)		4.12 Ω
Rotor resistance (R_r)		8.79 Ω
Stator (ABC phase) leakage inductance (L_1)		0.0256 H
Stator (ABC phase) leakage inductance (L_2)		0.0256 H
Rotor leakage inductance (L_r)		0.043 H
Mutual inductance between two set of stator ((L_{lm})		0.0736 H
No of poles		4
Moment of inertia (J)		0.033 kg m^2
Frictional coefficient (B)		0.00722
a		249.39
b		0.7875
The constant in magnetization	A_1	550.81
characteristics of multi phase	A_2	0.0657
induction generator	A_3	25.0427
	A_4	0.0982
Shunt excitation capacitor		0.000070 F
Series excitation capacitor		0.000210 F
DC side capacitor (C_{DC})		1800e-06

References

1. M. G. Simoes and F. A. Farret, “Renewable energy systems design and analysis with induction generators”, CRC Press, Boca Raton, 2004.
2. K. Kurohane, T. Senjyu, A. Yona, N. Urasaki, T. Goya and T. Funabashi, *IEEE Trans. Smart Grid*, 2010, **I(2)**, 199.
3. H. Amimeur, D. Aouzellag, R. Abdessemed and K. Ghedamsi, *Trans. Electr. Power Energ. Syst*., 2012, **42(1)**, 60.
4. K. Strunz, E. Abbasi and D. N. Huu, *IEEE 1. Emerg. Sel. Topics Power Electron.*, 2014, **2(1)**, 115.
5. G. K. Singh, *Electric Power Systems Research*, 2004, **69**, 107.
6. G. K. Singh, *Electric Power Systems Research*, 2002, **61(2)**, 139.
7. D. Levy, *Electric Power Systems Research*, 1986, **11**, 205.
8. G. K. Singh and V. Pant, *Electric Machines and Power Systems*, 2000, **28**, 577.
9. Y. Li , Y. Hu and W. Huang, *et al*., *IEEE Trans. on Industrial Electronics*, 2009, **56(2)**, 530.
10. S. Basak and C. Chakraborty, *IEEE Trans. Ind. Electron*., 2015, **62(7)**, 4641.
11. M. Moradian and J. Soltani, *IEEE Trans. Energy Convers.*, 2016, **31(2)**, 531.
12. R. C. Bansal, T. S. Bhatti and D. P. Kothari, *IEEE Trans. Energy Convers.*, 2003, **18(3)**, 433.
13. R. C. Bansal, T. S. Bhatti and D. P. Kothari, *J. Inst. Eng.*, 2003, **83**, 262.
14. Li Yong, Hu Yuwen, Huang Wenxin, Zhang Yong,

HaoZhenyang and TengFulin, "Dual stator-winding induction generator based automotive power generation system using direct power control", IEEE Vehicle Power and Propulsion Conference, Harbin, 2008, 1.

15. D. Wang, W. Ma, F. Xiao, B. Zhang, D. Liu and A. Hu, *IEEE Trans. Energy Convers*., 2005, **20(4)**, 826.
16. F. Bu, W. Huang, Y. Hu, J. Shi and K. Shi, *IEEE Transactions on Power Electronics*, 2012, **27(1)**, 10.
17. P. Vadana and Sasi K. Kottayil, *Advances in Intelligent Systems and Computing*, 2016, **397**, 627.
18. Duran, J. Mario and Federico Barrero, *IEEE Transactions on Industrial Electronics*, 2016, **63(1)**, 459.
19. G. Renukadevi and K. Rajambal, W*aste International Journal of Electrical, Computer, Electronics and Communication Engineering*, 2012, **6(9)**.
20. C. Kalaivani and K. Rajambal, "Modeling and analysis of multiphase induction generator", Circuit, Power and Computing Technologies (ICCPCT), International Conference on IEEE, 2016.
21. P. C. Krause, "Analysis of Electric Machinery and Drive systems", Wiley IEEE Press, 2013. ISBN: 978-1-118-02429-4
22. S. Satpathy, N. K. Kishore, D. Kastha and N. C. Sahoo, *IEEE Trans. Energy Convers.*, 2014, **29(2)**, 418.
23. S. Hazra and P. S. Sensharma, *IET Renew. Power Gener*., 2010, **4(4)**, 383.
24. S. S. Singh and A. N. Tiwari, *Int. 1. Adv. Res. Electron. Commun. Eng. (IJARECE)*, 2013, **2(2)**, 214.
25. J. W. Simpson-Porco, Q. Shafiee, F. Dorfler, J. C. Vasquez, J. M. Guerrero and F. Bullo, *IEEE Trans. Ind. Electron.*, 2015, **62(11)**, 7025.
26. F. Bu, Y. Hu, W. Huang, S. Zhuang and K. Shi, *IEEE Trans. Power Electron*., 2014, **29(4)**, 1681.
27. F. Bu, Y. Hu, W. Huang, S. Zhuang and K. Shi, *IEEE Trans. Power Electron*., 2015, **30(2)**, 561.
28. H. Xu, F. Bu, W. Huang, Y. Hu, H. Liu and Y. Zhao, *IEEE Trans. Emerg. Sel. Topics Power Electron*., 2016, **4(3)**, 1007.